Journal of Alloys and Compounds 489 (2010) 456–460

Contents lists available at ScienceDirect

Journal of Alloys and Compounds

journal homepage: www.elsevier.com/locate/jallcom

Characteristics of nano-sized silver–glass composite powders prepared by flame spray pyrolysis

Hye Young Koo, Jang Heui Yi, Yun Chan Kang*

Department of Chemical Engineering, Konkuk University, 1 Hwayang-dong, Gwangjin-gu, Seoul 143-701, Republic of Korea

ARTICLE INFO

Article history:
Received 16 July 2009
Accepted 7 September 2009
Available online 23 September 2009

Keywords:
Chemical synthesis
Gas–solid reaction

ABSTRACT

Nano-sized silver–glass composite powders were directly prepared by high-temperature flame spray pyrolysis applying ultrasonic spray generator. The silver–glass composite powders with various glass contents had nanometer size, spherical shape and non-aggregation characteristics. The mean size of the silver–glass composite powders was 56 nm. The nano-sized silver–glass composite powders had pure Ag crystal structures irrespective of adding amounts of glass. The silver conducting films formed from the nano-sized silver–glass composite powders had dense structures at firing temperatures between 400 and 500 °C. The silver conducting films formed from the nano-sized silver–glass composite powders had lower sheet resistivities than those formed from the nano-sized silver powders irrespective of the firing temperatures. The sheet resistivities of the silver conducting films formed from the nano-sized silver–glass composite powders with 1 wt% glass content were 53, 16 and 11 mΩ/sq at firing temperatures of 400, 450 and 500 °C, respectively.

1. Introduction

Silver conducting films have applied extensively for making electrical contacts in solar cells, hybrid circuits and other devices due to their excellent electrical properties [1–3]. Development of low firing temperature silver paste will improve the characteristics of silver conducting thick films. Melting temperature of silver decreased with decrease of the powders. Therefore, nano-sized silver powders are applied to decrease the firing temperature of silver conducting films [4–6]. Ink-jet printing as the fabrication technology of conductive films also requires the nano-sized silver powders [6]. Nano-sized glass powders are also required to develop the nano-silver paste. Glass powers act as a permanent binder and also promote sintering of metal powders during the sintering process and enable binding of the functional film to the substrate [7,8].

Nano-sized silver powders have been developed by various liquid solution and gas phase reaction methods [9–14]. However, nano-sized glass powders for silver conducting films have not been well developed. Metal–metal and metal–ceramic composite powders have been extensively studied to improve the properties of pure metal powders [15–18]. However, metal–glass composite powders have not been studied well because of the different preparation process of metal and glass powders.

In this study, silver–glass composite powders were directly prepared by high-temperature flame spray pyrolysis applying ultrasonic spray generator. The silver–glass composite powders with various glass contents had nanometer size, spherical shape and non-aggregation characteristics. The characteristics of silver conducting films formed from the nano-sized silver–glass composite powders were investigated.

2. Experimental procedure

Silver–glass composite powders were directly prepared by flame spray pyrolysis. The composition of glass material was 14.8 wt% ZnO–77.4 wt% Bi_2O_3–6 wt% B_2O_3. Small amount of BaO, Al_2O_3, Na_2O and SiO_2 were added. Glass contents of the composite conducting powders were changed from 1 to 6 wt% of silver component. The system of flame spray pyrolysis has a droplet generator, flame nozzle, quartz reactor, powder collector, and blower. A 1.7 MHz ultrasonic spray generator with 6 resonators is used to generate droplets, which are carried into the high-temperature diffusion flame by oxygen, as the carrier gas. Droplets or powders evaporate, decompose, and melt inside the diffusion flame. Propane as the fuel and oxygen as the oxidizer create the diffusion flame. The flame nozzle has five concentric pipes. Droplets generated from the precursor solution are supplied to the diffusion flame through the center pipe by different flow rates of carrier gas. The flow rates of fuel, oxidizer and carrier gases were each 5, 40, and 20 L/min. The volume ratio of ethyl alcohol/distilled water in the mixed solvent was 1/3. The spray solutions were obtained by adding $Ag(NO_3)$, ZnO (Kanto, 99%), Bi_2O_3 (Junsei, 99%), H_3BO_3 (Kanto, 99.5%), $Ba(NO_3)_2$ (Junsei, 99%), $Al(NO_3)_3{\cdot}9H_2O$ (Junsei, 98%), Na_2CO_3 (Kanto, 99%) and tetraethyl orthosilicate (TEOS, Aldrich, 98%) to distilled water using appropriate amount of nitric acid. The overall solution concentration of metal components composing the silver–glass composite powders was fixed to 0.5 M.

The crystal structures of the silver–glass composite powders were studied using X-ray diffraction (XRD, RIGAKU, D/MAX-RB) with Cu Kα radiation ($\lambda = 1.5418 \times 10^{-10}$ m). The morphologies of the silver–glass composite powders

* Corresponding author. Tel.: +82 2 2049 6010; fax: +82 2 458 3504.
E-mail address: yckang@konkuk.ac.kr (Y.C. Kang).

0925-8388/$ – see front matter © 2009 Elsevier B.V. All rights reserved.
doi:10.1016/j.jallcom.2009.09.084

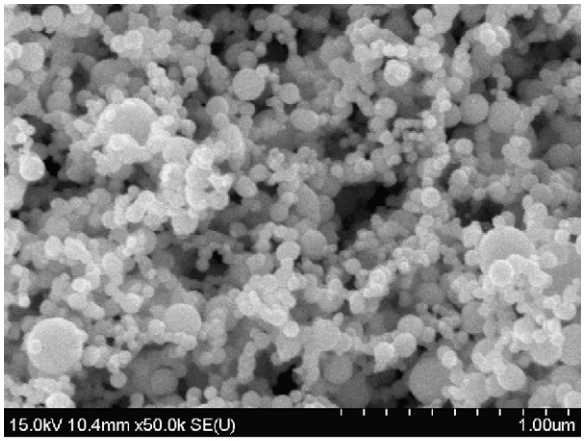

(a) Pure silver

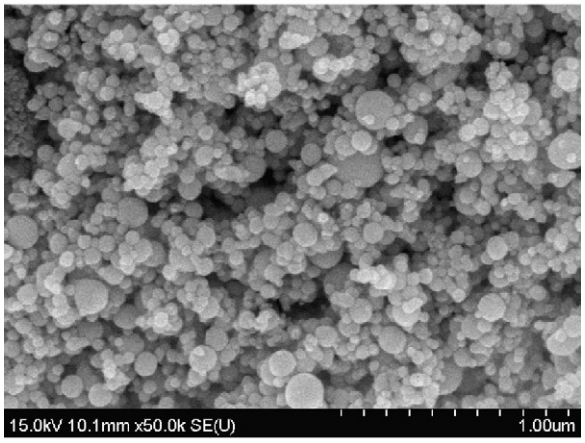

(b) Silver-glass composite

Fig. 1. FE-SEM images of the nano-sized pure silver and silver–glass composite powders. (a) Pure silver and (b) silver–glass composite

were investigated using field emission scanning electron microscopy (FE-SEM, HITACHI, S-4800) and transmission electron microscopy (TEM, JEOL, JEM-2010). The morphological characteristics of the silver conducting films were investigated by scanning electron microscopy (SEM, JEOL, JSM-6060). The sheet resistivities of the silver conducting films were measured using four point prove method (CMT-SR 1000N, Advanced Instrument Technology).

3. Results and discussion

Fig. 1 shows the morphology characteristics of the nano-sized pure silver and silver–glass composite powders prepared by flame spray pyrolysis. Glass content of the silver–glass composite powders was 3 wt% of silver component. The pure silver and silver–glass composite powders as shown in the FE-SEM images have nanometer sizes. Pure silver powders have slightly aggregated structure between the powders. On the other hand, the silver–glass composite had non-aggregation characteristics as shown in Fig. 1(b). The mean sizes of the pure silver and silver–glass composite powders measured from the FE-SEM images were 81 and 56 nm.

Fig. 2 shows the low and high resolution TEM images of the silver–glass composite powders prepared by flame spray pyrolysis. The silver–glass composite powders had nanometer size and spherical shape. Glass phase with amorphous structure as shown by arrows in Fig. 2(b) covered the nano-sized silver powders. Nano-sized silver–glass composite powders had core–shell structure.

Droplets generated by ultrasonic nebulizer had several microns size. Therefore, silver or glass powders prepared by ultrasonic spray pyrolysis had submicron sizes because one particle was formed from one droplet. However, silver–glass composite powders prepared by high-temperature flame spray pyrolysis had nanometer sizes. Evaporation of silver and glass components occurred inside the high-temperature diffusion flame. Nano-sized powders were formed by nucleation and growth mechanisms from the evaporated vapors of silver and glass components. Melting and quenching processes of the powders produced the composite powders with core–shell structure. Separation of silver and glass components occurred during the melting and quenching processes of the composite powders. Fig. 3 shows the formation mechanism of the nano-sized silver–glass composite powders in the flame spray pyrolysis.

Fig. 4 shows the XRD patterns of the pure silver and silver–glass composite powders. The composite conducting powders had pure Ag crystal structures irrespective of adding amounts of glass. The mean crystallite sizes of the nano-sized composite powders were measured by Scherrer's equation. The mean crystallite size of the pure silver powders was 24 nm. However, the mean crystallite sizes of the nano-sized silver–glass composite powders with 1 and 6 wt% glass contents were 24 and 22 nm, respectively.

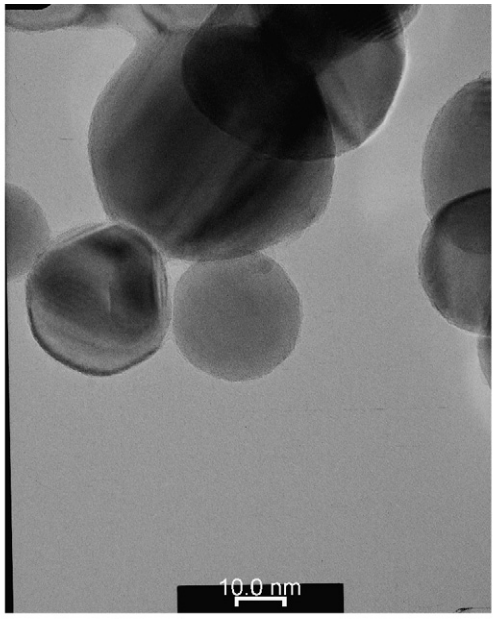

(a) low resolution TEM

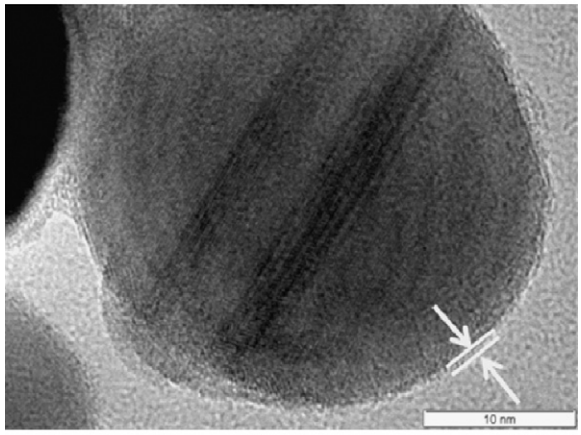

(b) high resolution TEM

Fig. 2. TEM images of the nano-sized silver–glass composite powders. (a) Low resolution TEM and (b) high resolution TEM.

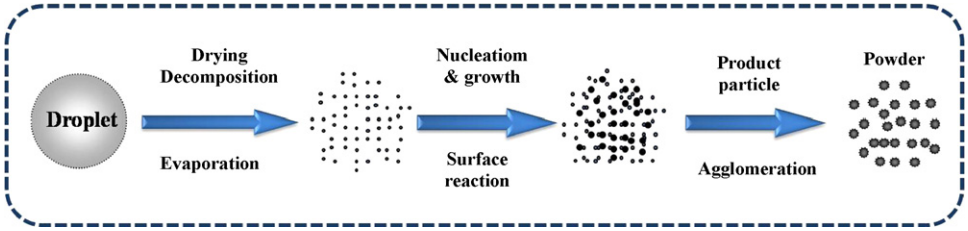

Fig. 3. Formation mechanism of the nano-sized silver–glass composite powders in the flame spray pyrolysis.

The nano-sized silver–glass composite powders with various glass contents prepared by flame spray pyrolysis were mixed with an organic vehicle. The paste was screen-printed onto the soda-lime glass substrate. The printed glass substrate was dried at 120 °C for 30 min in order to remove solvent. The dried glass substrate was fired by 2 steps. In the first step, the glass was fired at 350 °C for 30 min with a heating rate of 5 °C/min and in the second step, the glass substrate was fired at temperatures of 400, 450 and 500 °C for 10 min under same condition. Fig. 5 shows the SEM images of the surfaces of the silver conducting films fired at various temperatures. Glass content of the silver–glass composite powders was 3 wt% of silver component. Melting of the nano-sized silver–glass composite powders occurred at a low firing temperature of 400 °C. Grain growth of the silver conducting films occurred according to the increase of the firing temperatures.

Fig. 6 shows the SEM images of the cross sections of the silver conducting films formed from the silver–glass composite powders with various glass contents. The firing temperature was 400 °C. The silver conducting film formed from the nano-sized silver–glass composite powders with 1 wt% glass content had porous structure. On the other hand, the silver conducting films formed from the nano-sized silver–glass composite powders with 3 and 6 wt% glass contents had dense structures and high adhesion strength to the glass substrate. The thicknesses of the silver conducting films formed from the nano-sized silver–glass composite powders with 1, 3 and 6 wt% glass contents were 2.9, 2.3 and 2.2 μm. Glass material of the powders improved the firing characteristics of the composite powders.

Fig. 7 shows the sheet resistivities of the silver conducting films formed from the nano-sized pure silver and silver–glass composite powders prepared by flame spray pyrolysis. The silver conducting films formed from the nano-sized silver–glass composite powders had lower sheet resistivities than those formed from the nano-sized silver powders irrespective of the firing temperatures. The sheet resistivities of the silver conducting films decreased with

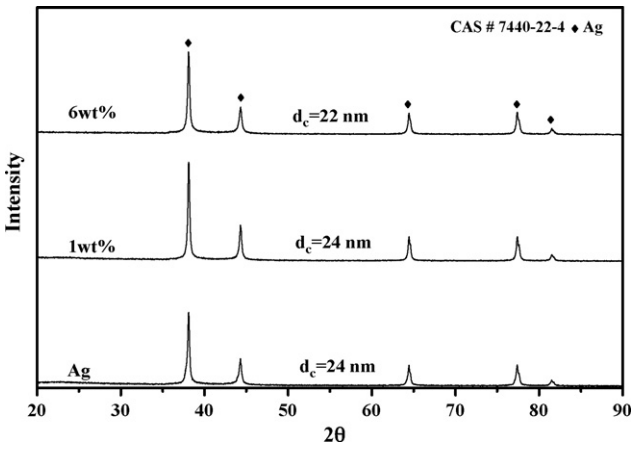

Fig. 4. XRD patterns of the pure silver and silver–glass composite powders.

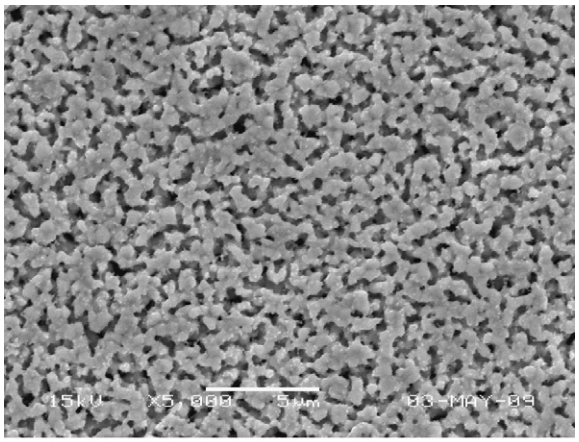

(a) 400 °C

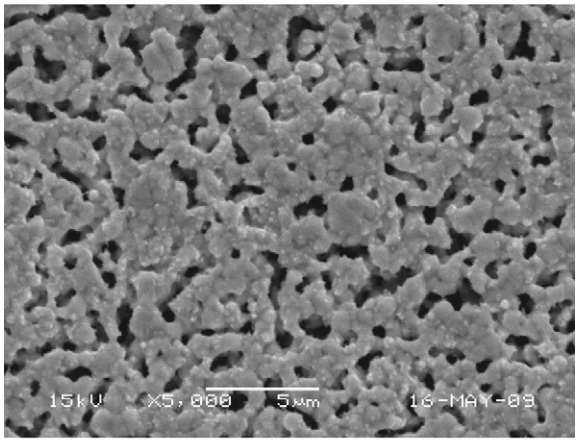

(b) 450 °C

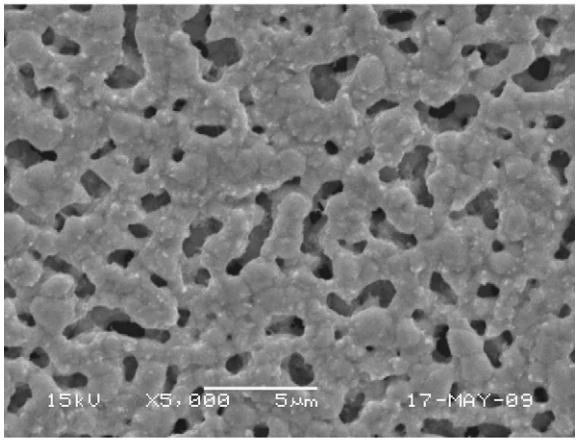

(c) 500 °C

Fig. 5. SEM images of the surfaces of the silver conducting films formed from the nano-sized silver–glass composite powders. (a) 400 °C, (b) 450 °C and (c) 500 °C.

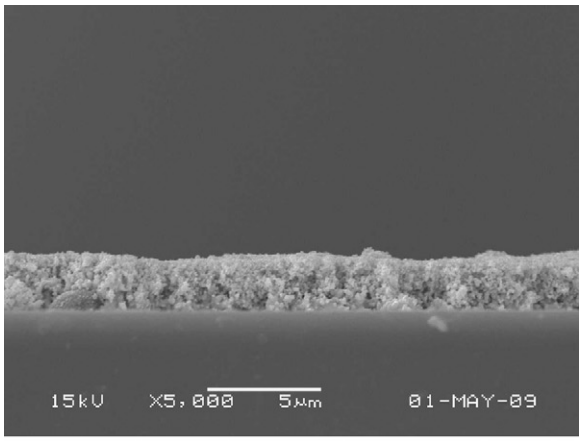

(a) 1 wt%

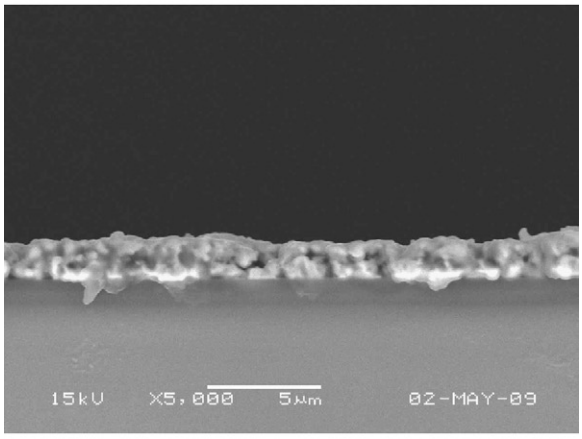

(b) 3 wt%

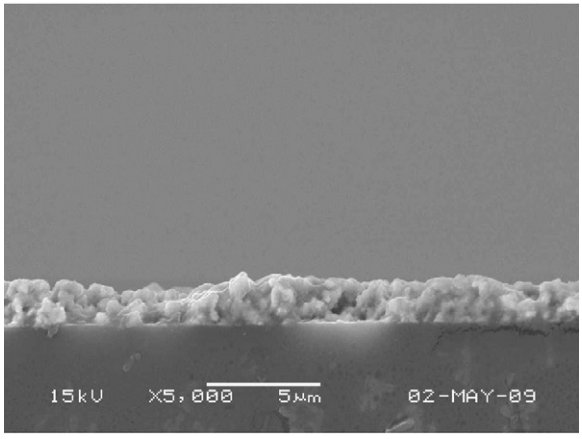

(c) 6 wt%

Fig. 6. SEM images of the cross sections formed from the nano-sized silver–glass composite powders with various glass contents. (a) 1 wt%, (b) 3 wt%, and (c) 6 wt%.

increasing firing temperatures irrespective of the glass content of the nano-sized silver–glass composite powders. However, the optimum glass content of the nano-sized silver–glass composite powders to obtain the silver conducting films with low sheet resistivities was changed according to the firing temperatures. The sheet resistivities of the silver conducting films fired at 400 °C decreased with increasing glass content of the nano-sized silver–glass composite powders. The sheet resistivities of the silver conducting films formed from the nano-sized silver–glass composite powders with 1 and 6 wt% glass were 53 and 30 mΩ/sq at a firing

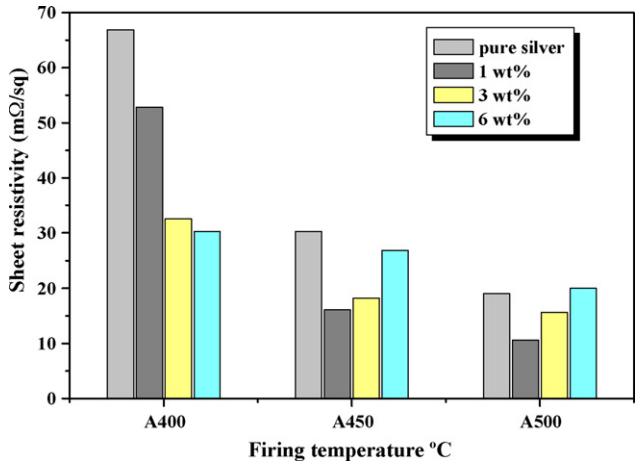

Fig. 7. Sheet resistivities of the silver conducting films formed from the pure silver and silver–glass composite powders.

temperature of 400 °C. The silver conducting films formed from the nano-sized silver–glass composite powders with 1 wt% glass content had the lowest sheet resistivities as 16 and 11 mΩ/sq at firing temperatures of 450 and 500 °C. However, the sheet resistivities of the silver conducting films formed from the nano-sized silver–glass composite powders with 6 wt% glass content were 27 and 20 mΩ/sq at firing temperatures of 450 and 500 °C, respectively. Nano-sized silver–glass composite powders had good firing characteristics because of homogeneous distribution of silver and glass components. Therefore, the silver conducting films formed from the nano-sized silver–glass composite powders with low glass content had low sheet resistivities at firing temperatures of 450 and 500 °C.

4. Conclusions

Nano-sized silver–glass composite powders with various glass contents were directly prepared by flame spray pyrolysis. Nano-sized silver–glass composite powders had good firing characteristics at temperatures between 400 and 500 °C. Silver conducting films formed from the nano-sized silver–glass composite powders had dense structures and low sheet resistivities. The optimum glass contents of the nano-sized silver–glass composite powders to obtain the silver conducting films at firing temperatures of 450 and 500 °C were low as 1 wt% of silver component because of good firing characteristics of powders. The silver conducting films formed from the nano-sized silver–glass composite powders had low sheet resistivities at firing temperatures between 400 and 500 °C.

Acknowledgement

This work was supported by Seoul R & BD Program (WR090671).

References

[1] R.W. Vest, Ceram. Bull. 65 (1986) 631.
[2] S.B. Rane, T. Seth, G.J. Phatak, D.P. Amalnerkar, B.K. Das, Mater. Lett. 57 (2000) 3096.
[3] J.D. Provance, K. Allison, Proc. Int. Symp. Hybrid Microelectron. 6 (1983) 60.
[4] K.J. Park, D.S. Seo, J.K. Lee, Colloid Surf. A 313–314 (2008) 351.
[5] S.H. Park, D.S. Seo, J.K. Lee, Colloid Surf. A 313–314 (2008) 197.
[6] D.H. Jang, D.J. Kim, B.Y. Lee, S.S. Kim, M.S. Kang, D.K. Min, J.H. Moon, Adv. Funct. Mater. 18 (19) (2008) 2862.
[7] P.F. Becher, W.L. Newell, J. Mater. Sci. 12 (1997) 90.
[8] T.T. Hitch, J. Electron. Mater. 3 (1974) 553.
[9] W. Li, S. Seal, E. Megan, J. Ramsdell, K. Scammon, G. Lelong, L. Lachal, K.A. Richardson, J. Appl. Phys. 93 (2003) 9553.

[10] P.K. Khanna, N. Singh, D. Kulkarni, S. Deshmukh, S. Charan, P.V. Adhyapak, Mater. Lett. 61 (2007) 3366.
[11] W. Zhang, X. Qiao, J. Chen, Mater. Sci. Eng. B 142 (2007) 1.
[12] H. Keskinen, J.M. Mäkelä, M. Vippola, M. Nurminen, J. Liimatainen, T. Lepistö, J. Keskinen, J. Mater. Res. 19 (5) (2004) 1544.
[13] J.M. Mäkelä, H. Keskinen, T. Forsblom, J. Keskinen, J. Mater. Sci. 39 (2004) 2783.
[14] A.I. Korchagin, Vacuum 77 (2005) 485.
[15] N. Iida, K. Nakayama, I.W. Lenggoro, K. Okuyama, J. Soc. Powder Technol. 38 (2001) 542.
[16] N. Aoyagi, T. Ookawa, R. Ueyama, N. Ogata, T. Ogihara, J. Ceram. Soc. Jpn. 112 (2004) S891.
[17] T.C. Pluym, T.T. Kodas, L.M. Wang, H.D. Glicksman, J. Mater. Res. 10 (1995) 1661.
[18] M. Matsumoto, K. Kaneko, Y. Yasutomi, S. Ohara, T. Fukui, Y. Ozawa, J. Ceram. Soc. Jpn. 110 (2002) 60.